Materials Chemistry and Physics 122 (2010) 582–587

Contents lists available at ScienceDirect

Materials Chemistry and Physics

journal homepage: www.elsevier.com/locate/matchemphys

Role of valence state of dopant (Eu^{2+}, Eu^{3+}) and growth environment in luminescence and morphology of $SrAl_{12}O_{19}$ nano- and microcrystals

Santa Chawla*, Ashish Yadav

National Physical Laboratory, Dr. K.S. Krishnan Road, New Delhi 110012, India

ARTICLE INFO

Article history:
Received 21 July 2009
Received in revised form 11 March 2010
Accepted 19 March 2010

Keywords:
Inorganic compounds
Photoluminescence spectroscopy
Microstructure

ABSTRACT

Incorporation of europium luminescent centre in its chosen valence state Eu^{2+} or Eu^{3+} has been effectively done in the complex strontium hexa aluminate $SrAl_{12}O_{19}$ by high temperature solid state reaction at regulated environment. Nanocrystalline $SrAl_{12}O_{19}$ doped with europium in its reduced form Eu^{2+}, could be successfully synthesized by controlled autocombustion process from the nitrate salts of precursor components. The charge state of the dopant ion was ascertained from photoluminescence studies which show series of sharp emission lines in 590–710 nm range for Eu^{3+} activator whereas broad green emission for Eu^{2+} activator. Nanocrystalline $SrAl_{12}O_{19}$:Eu showed blue shifted broad green emission characteristic of Eu^{2+} 4f5d transition demonstrating the effectiveness of autocombustion process in producing Eu^{2+} charge state which usually requires a reducing environment. Intra-band gap excitation of $SrAl_{12}O_{19}$ between energy levels of rare earth dopant could be tailored effectively to obtain broad excitation transition in near UV/violet region and emission in the visible region. Striking dependence of morphology on valence state of Eu and growth environment was observed which could be explained due to creation of solid state defects in formation of lamellar structure in oxygen-rich environment.

1. Introduction

Alkaline earth hexa aluminate $SrAl_{12}O_{19}$ is a unique host with large band gap (7.6 eV) which has shown quantum splitting behaviour with Pr^{3+} doping [1], good laser properties with $Pr^{3+}$and Nd^{3+} doping [2] and strong green emission suitable for plasma display panel applications with Mn doping [3]. The rare earth dopant in $SrAl_{12}O_{19}$ experiences very weak crystal field due to large coordination number of Sr atom (12) and long nearest neighbour distances (2.750–2.785 Å), giving rise to very sharp emission lines for trivalent rare earth dopants. As alkaline earth aluminates have a large bandgap, they form a suitable host material for doping rare earth ions and have been a topic of research for obtaining suitable emission with high quantum efficiency. Strontium aluminates doped with rare earth ions were observed to be efficient light emitter and found many applications as long after glow phosphor [4]. For most applications, however, $SrAl_2O_4$ has been used [5]. Strontium hexaaluminate doped with Eu^{2+} has shown 90% quantum efficiency for blue emission and while codoped with Cr^{3+} showed energy transfer from Eu^{2+} to Cr^{3+} [6]. Eu has been used widely as luminescent centre in both its valence state Eu^{2+} and Eu^{3+} in different hosts to obtain efficient light emission ranging from blue to red. As $SrAl_{12}O_{19}$ host has exhibited very interesting light emitting properties, the present work explores the suitability of Europium-doped binary hexa-aluminate $SrAl_{12}O_{19}$ as an efficient phosphor for light emitting devices and controlled tuning of the emission depending upon growth conditions. This is possible because transitions within $^5D_0$ configuration of rare earth ions in solids are predominately of electric dipole nature and made possible by the mixing of the $^5D_0$ states with the $^5D_0$–^7F states. In the present study, $SrAl_{12}O_{19}$ doped with rare earth activator Eu in both its charge states Eu^{2+} and Eu^{3+} in its bulk as well as nanocrystalline form has been synthesized. Doping with either of two valence states of europium i.e., Eu^{2+} or Eu^{3+} has been studied with respect to photoluminescence and morphology of the micro- and nanocrystals of $SrAl_{12}O_{19}$. Photoluminescence excitation and emission spectra were investigated to explore the possibility of using these phosphors for solid state lighting applications using near UV/blue LED as well as possible use as a solar cell phosphor to convert the unutilized part of solar spectrum (UV–blue) to wavelength suitable for absorption by silicon solar cell [7].

2. Experimental

2.1. Synthesis of $SrAl_{12}O_{19}$:Eu phosphors

Strontium hexa aluminate ($SrAl_{12}O_{19}$) was prepared from stoichiometric proportions of high purity $SrCO_3$, Al_2O_3. Percentage of dopant Eu was 2 mol% and was added as Eu_2O_3. Additional flux of boric acid was added for better crystallinity. All the components were thoroughly ground and mixed. The phosphor $SrAl_{12}O_{19}$:Eu was

* Corresponding author. Tel.: +91 11 45609242; fax: +91 11 45609310.
E-mail address: santa@nplindia.org (S. Chawla).

0254-0584/$ – see front matter © 2010 Elsevier B.V. All rights reserved.
doi:10.1016/j.matchemphys.2010.03.050

synthesized by solid state reaction [1,8] in both oxidizing and reducing atmospheres to obtain different valence states of Eu in the host lattice. In the first experiment, the mixture was calcined in a furnace at 1300 °C in air for 2 h. In the second experiment carbon powder was added and the mixture was calcined in reducing atmosphere (nitrogen and ammonia) at 1300 °C also for 2 h and allowed to cool slowly in reducing atmosphere. Fired sample was ground to a fine powder.

Nanocrystalline $SrAl_{12}O_{19}$ doped with europium was prepared by controlled autocombustion process [9]. All the precursor components were taken in stoichiometric proportions from the nitrate salts of precursor components. To achieve this, all the oxide precursors including the rare earth component were changed into their nitrate salt by suitable reaction with nitric acid. A solution in deonized water of all the nitrate precursors e.g., $Sr(NO_3)_3$, $Al(NO_3)_3$, $Eu(NO_3)_3$ together with the fuel urea was put into a cylindrical quartz beaker and heated to dehydrate. As the solution thickened, the beaker was closed with a quartz lid. With continued heating, the solution bubbled and expanded and at a certain instance autocombustion of urea took place with fire being ignited within the beaker. The exothermic reaction completed in few minutes with the resultant fluffy voluminous white mass of the complex oxide compound $SrAl_{12}O_{19}$:Eu.

2.2. Characterization

Phase characterization was done by X-ray diffraction on a Rigaku Miniflex X-ray diffractometer using Cu-Kα radiation (λ = 1.54 Å). The morphology analysis was performed using a LEO 440 PC based digital scanning electron microscope. Measurement of photoluminescence (PL) emission and excitation spectra and time resolved decay were done with Edinburgh Instruments FLSP920 combined steady state and time resolved fluorescence spectrometer using xenon lamp source.

3. Results and discussion

3.1. Structure and morphology

X-ray diffraction pattern (Fig. 1a) shows the Bragg diffraction peaks of europium-doped $SrAl_{12}O_{19}$ phosphor synthesized by solid state reaction method. The two samples of $SrAl_{12}O_{19}$ synthesized in air and reducing atmosphere exhibit almost identical XRD patterns corresponding to the pure hexagonal magnetoplumbite phase of $SrAl_{12}O_{19}$. The XRD peaks of doped and undoped $SrAl_{12}O_{19}$ are similar since the level of impurity doping is low (2 mol%) in the $SrAl_{12}O_{19}$ host lattice. All the peaks could be indexed to magnetoplumbite $SrAl_{12}O_{19}$ phase, matching perfectly with the JCPDS Card No.26-976. The phase identification of the nanocrystalline sample prepared by autocombustion method (Fig. 1b) also confirm the magnetoplumbite structure showing the effectiveness of relatively low temperature synthesis process in forming the complex hexa aluminate structure. The crystallographic parameters of synthesized nano- and microcrystallite of $SrAl_{12}O_{19}$ have been compared with standard JCPDS values and listed in Table 1. The average crystallite size estimated using Scherrer formula is 23 nm for the nanocrystalline form prepared by autocombustion method. As dopant concentration is only 2 mol%, the lattice strain of the host lattice is not appreciable and Scherrer formula provides a reasonable estimate of average crystallite size.

SEM micrograph of $SrAl_{12}O_{19}$:Eu^{3+} sample fired in air is shown in Fig. 2a which shows lamellar structure. The SEM micrograph of

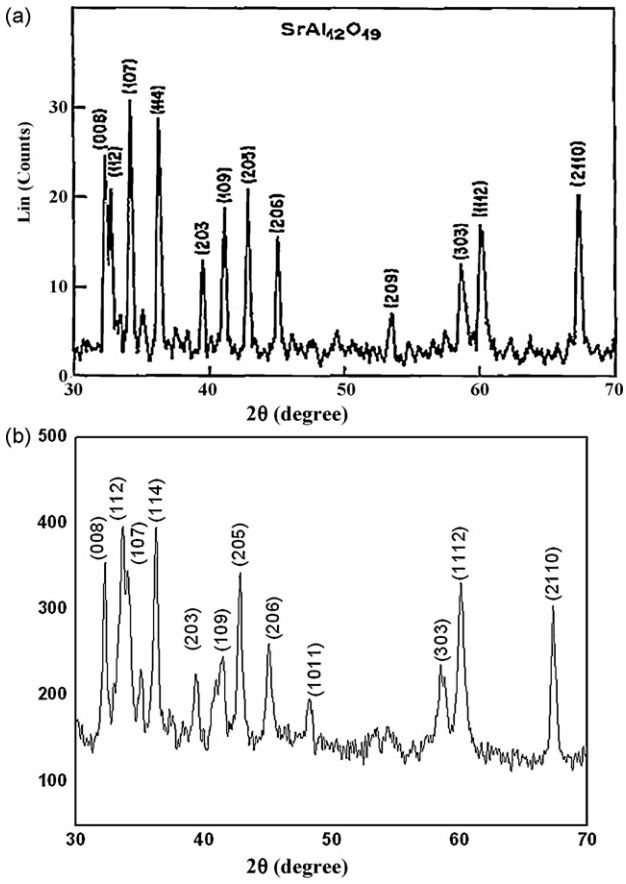

Fig. 1. XRD pattern of $SrAl_{12}O_{19}$:Eu prepared by (a) solid state synthesis (b) autocombustion method. All the peaks are indexed to magnetoplumbite $SrAl_{12}O_{19}$ phase.

$SrAl_{12}O_{19}$:Eu^{2+} sample fired in reducing atmosphere (Fig. 2b) show well-formed rounded particles resembling hexagonal shape. The striking change in morphology has its origin in growth environment and the valence state of Eu ions in the host lattice. In samples fired in air, Eu gets incorporated as Eu^{3+} whereas in samples fired in reducing atmosphere, Eu^{3+} is reduced to Eu^{2+} state. The signature of the valence state of Eu is confirmed from Photoluminescence (PL) spectra as shown in Fig. 3(b). Dopant Eu^{2+}/Eu^{3+} are accommodated in substitutional sites of Sr^{2+}. The radius of host Sr^{2+} (0.118 nm) is similar to substitutional Eu^{2+} (0.117 nm) but differ from Eu^{3+} (0.947 nm). For dopant in the divalent state (Eu^{2+}), overall charge compensation in the lattice could be fulfilled by one to one substitution. For Eu^{3+} dopant, charge compensation would require that two Eu^{3+} ions are substituted for three Sr^{2+} ions [10]. For Eu^{3+} dopant state, there could be two ways to maintain overall charge neutral-

Table 1
Crystallographic parameters of $SrAl_{12}O_{19}$ synthesized in different environments.

Value of *hkl*	*d* values (JCPDS data)	SSR in reducing atmosphere	SSR in air atmosphere	Autocombustion
008	2.7600	2.7706		
107	2.6400		2.6200	2.6600
114	2.4900	2.4725	2.4729	2.4807
112	2.7100	2.7300		2.7233
110	2.7950			2.7810
203	2.3000	2.2817	2.2800	2.2918
109	2.1850	2.1940		2.1880
205	2.1200	2.1058	2.1063	2.1130
206	2.0220	2.0069	2.0781	2.0128
303	1.5720	1.5725	1.5724	1.5706
1112	1.5360	1.5354	1.5361	1.5362
2110	1.4080	1.3880	1.4018	1.3912
209	1.7230	1.7114	1.7103	